

## Oriented Z-Type Langmuir–Blodgett Films from a Soluble Asymmetrically Substituted Polydiacetylene

Dong-Wook Cheong,<sup>†</sup> Woo-Hong Kim,<sup>†</sup> Lynne A. Samuelson,<sup>‡</sup> Jayant Kumar,<sup>§</sup> and Sukant K. Tripathy<sup>\*,†</sup>

Center for Advanced Materials, Department of Chemistry and Physics, University of Massachusetts Lowell, Lowell, Massachusetts 01854, and Biotechnology Division, U.S. Army Natick Research, Development, and Engineering Center, Natick, Massachusetts 01760

Received August 21, 1995; Revised Manuscript Received November 6, 1995<sup>®</sup>

**ABSTRACT:** A soluble, asymmetric polydiacetylene has been shown to form stable monolayers at the air–water interface of a Langmuir trough. The monolayers of this unconventional amphiphilic polymer could be repeatedly deposited onto hydrophobic substrates during every upstroke cycle of the vertical dipping method to form uniform Z-type multilayers. Characterization of the precise orientation of the polymer main chain has been carried out to determine the spatial correlation between the nonlinear optical chromophore responsible for second-order nonlinear optical properties and the backbone. Polarized UV/vis and IR spectroscopic studies indicate a preferential orientation of the main chain along the dipping direction with a mean fluctuation of  $\pm 30^\circ$  between director axis and chain trajectories. Polarization-dependent second-harmonic generation (SHG) in multilayers indicates a high degree of orientational anisotropy of the backbone. As expected, SHG intensities increase with the number of layers due to the noncentrosymmetric Z-type structure. The second-order nonlinear coefficient ( $d_{33}$ ) was estimated to be 1.52 pm/V at 1064 nm of Nd:YAG laser after correcting for absorption. Surface characterization and alignment of the extended chain backbones is further established using atomic force microscopy (AFM).

### Introduction

Nonlinear optical (NLO) materials<sup>1</sup> have received considerable attention for a wide range of potential applications, such as electro-optic modulation, optical wave guides for frequency conversion, and all-optical switching. Inorganic crystals like LiNbO<sub>3</sub> and KDP have long been used as NLO materials in optoelectronic and photonic devices. These materials, however, require time-consuming crystal growth, polishing, and processing procedures for device fabrication. Substantial efforts<sup>1–3</sup> have been directed at organic polymeric NLO materials development to overcome some of these difficulties. Organic NLO materials can be readily synthesized by well-established methods, and design principles are emerging to enhance the optical nonlinearities. Polymers as NLO materials<sup>3</sup> have the added advantages of easier processability and low dielectric constants compared to the conventional inorganic crystals.

When discussing nonlinear optical processes, mainly second- and third-order effects are emphasized. The former requires noncentrosymmetry in the bulk along with a large molecular hyperpolarizability in individual molecular units. The noncentrosymmetry requisite for the second-order effects can be achieved through the preferred ordering of polar molecules by various methods such as single crystal growth, electric field poling, use of chiral molecules, and Langmuir–Blodgett (LB) or self-assembly (SA) techniques.

The LB technique may be used to construct noncentrosymmetric structures of molecules with interesting optical properties by taking advantage of the inherent self-assembling nature of the system.<sup>4</sup> Noncentrosymmetry can be achieved by either Z-type deposition of multilayers or molecular tailoring<sup>5</sup> in order to favor the

Z-type deposition process. Ashwell et al.<sup>6</sup> have demonstrated the quadratic dependence of the second harmonic intensity on the number of layers in the case of quinolinium zwitterion Z-type multilayers. Kunitake et al.<sup>7</sup> have also reported SHG from wholly  $\pi$ -conjugated oligo(phenylenevinylene)sulfonamides.

In the past, Z-type LB films, consisting of small molecules, have shown the inherent disadvantages of both disordering with increasing number of layers and light scattering due to the formation of microcrystalline domains.<sup>4,8</sup> Z-type (head to tail) structures in typical monomeric amphiphiles are intrinsically more unstable compared to Y-type structures (head to head or tail to tail), as they will ultimately try to reorient to form the Y-type.<sup>4</sup> Thus, an alternative approach is required to achieve the stable noncentrosymmetry in Z-type films. Deposition of a single polymeric material or alternating deposition of two different polymers containing NLO chromophores in alternate layers may provide the solution to this problem.<sup>9</sup> It is therefore desirable to consider polymeric multilayer systems with NLO chromophores which can provide improved structural stability and large nonlinear optical responses.<sup>10</sup>

Tieke and co-workers first reported<sup>11,12</sup> the solid-state polymerization of amphiphilic diacetylene monomers at the air–water interface. A number of monomeric diacetylenes<sup>12–14</sup> have since been used to form stable polymeric LB films. Polydiacetylenes (PDAs) are well-known  $\pi$ -conjugated systems with a quasi one-dimensional structure,<sup>15,16</sup> in which the delocalized  $\pi$ -electrons are considered to offer a unique electronic and optical anisotropy in single crystals of both monomers and polymers. Polydiacetylenes have emerged as important organic conjugated polymers with one of the highest third-order optical nonlinearities and ultrafast response times.<sup>16</sup> While third-order nonlinearities in polydiacetylenes have long been a major topic of research, only a few reports have been presented regarding the second-order nonlinearities. Large second- and third-order nonlinear optical effects have been demonstrated in liquid crystalline polydiacetylenes<sup>17</sup> where phase

\* Author for correspondence.

<sup>†</sup> Department of Chemistry, University of Massachusetts.

<sup>‡</sup> U.S. Army Natick Research, Development, and Engineering Center.

<sup>§</sup> Department of Physics, University of Massachusetts.

<sup>®</sup> Abstract published in *Advance ACS Abstracts*, January 15, 1996.

matching due to optical birefringence is indicated. Langmuir monolayers in both monomeric and polymeric diacetylenes have also shown second harmonic generation at the air–water interface due to the inherent noncentrosymmetry of a monolayer structure.<sup>18</sup>

We have recently reported on the design of various soluble, asymmetric diacetylene polymers<sup>19</sup> and characterized their nonlinear optical properties in bulk films.<sup>20</sup> One of these polydiacetylenes, poly{1-[[[(butoxycarbonyl)methyl]amido]oxy]-4-pyrimidyl}diacetylene or P-BPOD (shown in Inset of Figure 1), which possesses an asymmetric pyrimidyl ring and flexible urethane side groups, showed significant SHG in both spin-coated and cast films. This was achieved without electric field poling or any other external mechanism for preordering. In contrast, the well-established soluble poly(dibutyl 4,19-dioxo-5,18-dioxa-3,20-diaza-10,12-docosadienedioate) or poly-4-BCMU, as well as other symmetric PDA's, shows no SHG under similar processing conditions. Hence, SHG in P-BPOD may be explained by both asymmetry of the side groups and noncentrosymmetric alignment in the bulk through the intramolecular hydrogen bonding of the urethane linkages.<sup>20</sup> The molecular self-organization of P-BPOD appears to occur in transition from solution to solid as a film is cast. This phenomenon of self-assembly in the bulk is akin to the molecular self-assembly observed in liquid crystalline materials.<sup>20</sup> The nonlinear optical coefficient ( $d_{33}$ ) value measured in this system is comparable to that of the best reported values for ferroelectric liquid crystal systems. Self-assembled polydiacetylenes like P-BPOD may provide new opportunities to design  $\pi$ -conjugated NLO materials with high second- and third-order responses.

SHG detection in P-BPOD bulk films has led us to fabricate Langmuir–Blodgett (LB) films and study their nonlinear optical properties. In principle, the LB systems may result in enhanced ordering of the specific NLO chromophores and thereby increase the second-order susceptibility. Monolayers of P-BPOD molecules are quite stable at the air–water interface and may be deposited onto silanized (hydrophobic) glass substrates. Under optimized deposition conditions, multilayers have been transferred during every upstroke, without any deposition during the downstroke. To our knowledge, this is the first report of Z-type LB films in preformed polydiacetylene systems. This paper discusses SHG and the molecular orientation studies of these noncentrosymmetric Z-type LB films. Molecular orientation focusing on the features of the polymer backbone in these ordered LB films is studied by using spectroscopy (UV/vis and FTIR), NLO property measurements (both second and third order), and ellipsometry. AFM provides further information regarding molecular orientation and surface morphology.

## Experimental Section

A Langmuir film balance (MGW Lauda) was used to assemble the P-BPOD monolayer on pure water (Milli-Q) at 20 °C. The polymer solution, 0.5 mM prepared in chloroform (Aldrich, HPLC grade), was filtered using a 0.45  $\mu$ m Teflon membrane filter (VWR) and was then spread on the water subphase. After approximately 15 min, the monolayer was compressed at a speed of 1.0 cm<sup>2</sup>/s until collapse to obtain isotherms. The monolayer was held at a desired target pressure for transfer studies.

Hydrophilic glass substrates were prepared by cleaning the glass slides ultrasonically in Mallinckrodt Chem-Solv Lab cleaner and then in an air–plasma cleaner (Harrick Co.).

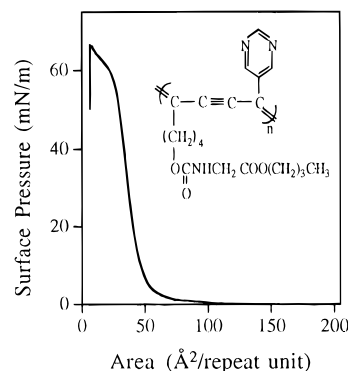


**Figure 1.** Pressure–area isotherm of P-BPOD from a water subphase at 20 °C. Inset is the chemical structure of P-BPOD.

Hydrophobic glass substrates were prepared by chemically treating the hydrophilic glass with octadecyltrichlorosilane (OTS, Aldrich). CaF<sub>2</sub> plates (Harrick Co.) were used without further surface treatment.

Optimization of film deposition conditions was carried out by varying both the surface pressure (15, 30, and 45 mN/m) and transfer speed (10, 5, and 2.5 mm/min). Reproducible, high-quality films were obtained in all cases under the following conditions. The monolayer was annealed on the subphase for 30 min at a constant pressure of 30 mN/m. The monolayer was very stable, as constant pressure could be maintained over several hours without any appreciable decrease in surface area. The rate of transfer was found to be optimum at 2.5 mm/min for the upstroke and 5 mm/min for the downstroke with an 18 min drying period between two consecutive dips for multilayer formation. The transfer ratios were typically 90–100% for each pass through the monolayer. Mono- and multilayer films were transferred onto hydrophobic plain glass substrates, hydrophobic glass substrates with a frosted slide, and CaF<sub>2</sub> plates for UV/vis spectroscopy, ellipsometry, and FT-IR spectroscopy, respectively. Polarized UV/vis absorption studies were carried out using a Perkin-Elmer Lambda 9 spectrophotometer with a polarizer. Vibration spectra were recorded using a Perkin-Elmer FT-IR spectrometer 1760 with a room-temperature TGS detector. A gold-wire polarizer (Perkin-Elmer) was set up for the polarization study. The thickness of the LB multilayers was measured using an AutoEL<sup>R</sup>-III automatic ellipsometer (Rudolph Research) with a He–Ne laser (632.8 nm).

SHG measurements were performed using a Q-switched Nd:YAG laser (1064 nm, pulse width 10 ns).<sup>20</sup> Third-order nonlinear optical effects were measured using the degenerate four-wave mixing (DFWM) technique.<sup>21</sup> A Nd:YAG laser of 1064 nm was frequency-doubled to provide 17 ps full width at half-maximum (FWHM) single pulses at 532 nm. These pulses were utilized to perform a DFWM experiment. AFM images of the LB films were obtained using an atomic force microscopy setup (Park Scientific Instruments, CA) with a Si<sub>3</sub>N<sub>4</sub> tip. Reproducible images were recorded and obtained with an applied force in the 10 nN range under well-calibrated conditions.

## Results and Discussion

**Langmuir–Blodgett Films.** The surface pressure–area isotherm ( $\pi/A$ ) of a P-BPOD monolayer exhibits an extremely steep rise (Figure 1), indicating formation of the solid condensed phase with little or no intermediate phase transitions. Well-known, soluble symmetric diacetylene polymer, poly-4-BCMU, shows a completely different isotherm with a phase transition which has been explained by significant conformational changes from monolayer to bilayer during compression at the air–water interface.<sup>22</sup> This behavior has been attributed to the hydrophilic interaction between the urethane–ester side groups and the aqueous subphase. Bilayer formation is attributed to the strong intramo-

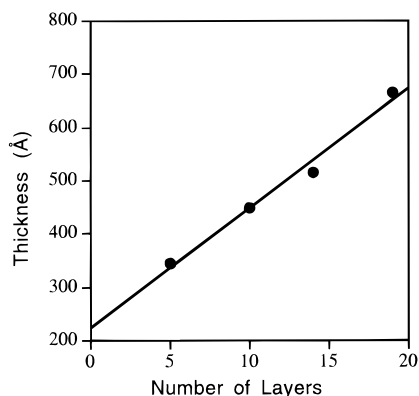


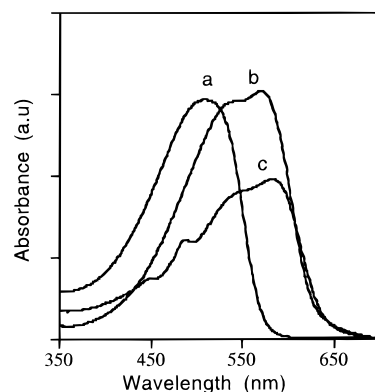
**Figure 2.** Thickness vs number of layers measured by ellipsometry.

lecular hydrogen bonds. The isotherm of P-BPOD shows only the condensed solid phase, with no observed monolayer to bilayer conformational transitions, as reported for poly-4-BCMU. It is believed that the asymmetry of the P-BPOD may provide relatively different hydrophilicity for pyrimidyl rings and urethane-ester linkages and that one side chain may lift up at the air-water interface to form a monolayer upon compression.

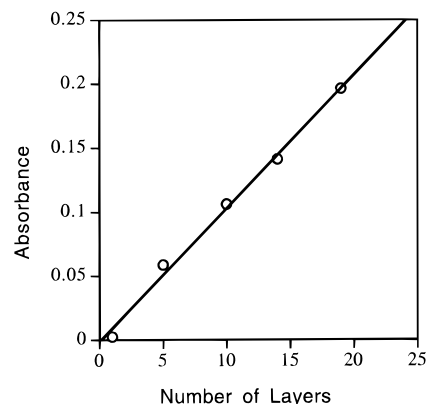
Extrapolation of the isotherm to zero pressure at the low-compressibility region gives a limiting area of approximately  $50 \text{ Å}^2$  per repeating unit. As shown in the inset of Figure 1, the chemical structure of P-BPOD consists of a diacetylene polymer backbone with two hydrophilic pendant groups (pyrimidyl ring and urethane-ester linkage). Given the slightly higher hydrophilic character of the urethane-ester linkages, it is more likely that these groups are in contact with the subphase, leaving both the terminal alkyl chains and slightly hydrophilic pyrimidyl ring groups protruding. This less than ideal amphiphilic orientation may contribute to the formation of unusual Z-type LB structures on transfer to hydrophobic substrates. This behavior would also preclude bilayer formation at the air-water interface, as seen in the case of BCMU. Multilayers could not be transferred onto hydrophilic substrates even after prolonged drying (several days) of the first layer. It could therefore be concluded that this unusual deposition behavior may be due to the nonclassical amphiphilic structure of P-BPOD molecules and partial hydrophilic interaction between successive layers.

**Characterization of LB Films.** Monolayer formation and structural order was further confirmed by ellipsometric measurements. Various multilayers were used to monitor the thickness of the film as a function of the number of layers (Figure 2). The average film thickness calculated from the slope<sup>23</sup> of this plot is  $20 \pm 3 \text{ Å}$ . Considering the theoretical length, of about  $25 \text{ Å}$ , for a fully extended P-BPOD molecule (broadside or monomer length in the polymer), the oriented backbone plane in a layer must be slanted with respect to the surface normal. A repeat unit length of  $5 \text{ Å}$  is assumed and a limiting area of approximately  $50 \text{ Å}^2$  per repeating unit is obtained from extrapolation of the curve to zero pressure at the low compressibility region from the isotherm.

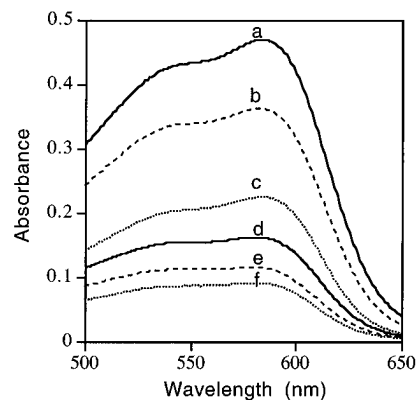
A comparison of the electronic absorption spectra of the solution, cast films, and LB multilayers is given in Figure 3. As expected, the maximum absorption wavelengths in both cast film ( $573 \text{ nm}$ ) and LB multilayers ( $583 \text{ nm}$ ) are red shifted as compared to that from the



**Figure 3.** Electronic absorption spectra of P-BPOD: (a) in solution ( $1.0 \text{ mM CHCl}_3$ ); (b) as cast film; (c) with LB 19 layers per side.



**Figure 4.** Electronic absorption vs number of layers at  $583 \text{ nm}$ .

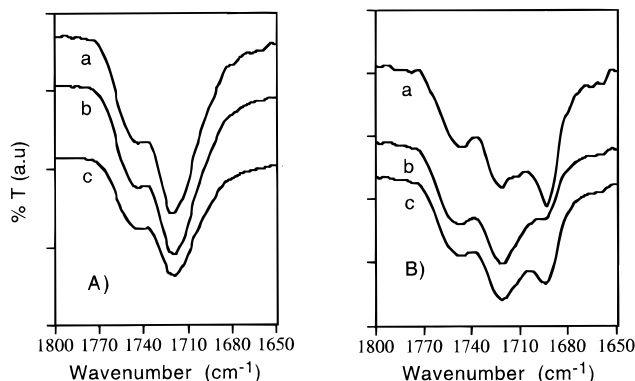


**Figure 5.** Polarized electronic absorption spectra of multilayers at normal incidence. Curves a-c are absorption ( $A_{\parallel}$ ) parallel and d-f are absorption perpendicular ( $A_{\perp}$ ) to the dipping direction in 19, 14, and 10 layers, respectively.

solution ( $509 \text{ nm}$ ). Since the wavelengths corresponding to  $\pi-\pi^*$  excitonic bands are related to the degree of order of the backbone, that is, the conjugation length, it is reasonable to state that the backbone conjugation length increases from coil-like conformations (in a thermodynamically good solution) to rigid-rod-like conformations (in both cast and LB films). A longer absorption band in the LB films compared to the cast films is therefore believed to be due to the enhanced backbone orientation. As shown in Figure 4, the peak absorption intensity increases at  $583 \text{ nm}$  with the number of layers. This linear increase of intensity with the number of layers implies reproducible, uniform, monolayer transfer during every upstroke.

**Table 1. Dichroic Ratios ( $R$ ) and Order Parameters ( $S$ ) in Various Multilayers**

LB films	1	5	10	14	19	cast film <sup>a</sup>
$R$	$2.85 \pm 0.05$	$3.15 \pm 0.04$	$2.79 \pm 0.09$	$3.17 \pm 0.06$	$2.90 \pm 0.07$	$1.01 \pm 0.03$
$S$	$0.35 \pm 0.01$	$0.42 \pm 0.02$	$0.37 \pm 0.01$	$0.47 \pm 0.05$	$0.38 \pm 0.02$	$0.01 \pm 0.005$

<sup>a</sup> Prepared from diluted CHCl<sub>3</sub> solution.**Figure 6.** Transmission FT-IR spectra for P-BPOD: (A) cast film on CaF<sub>2</sub>; (B) LB 19 layers per side on hydrophobic glass. (a–c) indicate the polarized spectra parallel and perpendicular to the dipping direction, and without polarization, respectively.

The main chains in a number of polymers during the LB film deposition process tend to align along the dipping direction. This orientation due to “polymer stretching” is reported to be a result of flow-induced orientation.<sup>24,25</sup> The degree of the polymer molecular orientation can be evaluated by electronic absorption dichroism, given that the polydiacetylene backbones present a characteristic and strong electronic transition. If the polydiacetylene backbone orients with respect to the dipping direction, the polarized electronic absorption parallel to the dipping direction ( $A_{||}$ ) will be stronger than that perpendicular to the dipping direction ( $A_{\perp}$ ).<sup>26</sup>

Figure 5 shows the polarized electronic absorption spectra of 10, 14, and 19 multilayers per side of substrate. In all cases, parallel absorption ( $A_{||}$ ) is significantly larger than perpendicular absorption ( $A_{\perp}$ ). If the dichroic ratio,  $R$ , is defined as  $A_{||}/A_{\perp}$ ,<sup>27</sup> the degree of orientation is characterized by  $R$  values. The  $R$  values for 1-, 5-, 10-, 14-, and 19-layer LB films are compared with those for the cast films, as shown in Table 1.  $R$  values in LB films range from 2.85 to 3.15, while the cast films show no significant linear dichroism. In addition, the main-chain orientation in rigid-rod-like polymer systems can be described by the two-dimensional order parameter ( $S$ ),<sup>26</sup> which can be expressed as  $S = (R - 1)/(R + 2)$ .  $S$  values of multilayers are also given in Table 1. As can be observed from Table 1, even though the order parameters are not extremely high (about 0.4), the conjugated backbones in LB films preferentially orient with respect to the dipping direction (in-plane anisotropy) during multilayer deposition, whereas the cast films are in-plane isotropic.

Using the results of the UV/vis linear dichroism studies, the orientation of the main chain can be estimated in terms of the mean deviation angle ( $\alpha$ ) between the main chain and the dipping direction. If the conjugated backbone is regarded as a quasi one-dimensional rigid-rod chain that induces the most intense  $\pi$ – $\pi^*$  electronic absorption, the angle  $\alpha$  can be determined using the dichroic ratio,  $\tan^2 \alpha = 1/R = A_{\perp}/A_{||}$ .<sup>29</sup> The angle distribution ( $\alpha$ ) lies in the range 29–

32°, indicating a small tilt of the main-chain orientation from the dipping direction.

Polarized Fourier-transform infrared spectroscopy (FT-IR) also provides valuable information regarding preferential absorption which occurs when the induced dipole moment direction of a particular vibration mode is matched to the electric vector of the polarized incident beam.<sup>29,30</sup> In a urethane bond-containing polydiacetylene such as poly-*n*-BCMU, hydrogen bonds occur only between adjacent carbonyl (C=O) and amino (N–H) groups of urethane bonds within a backbone, forming a coplanar structure between urethane side groups and the conjugated backbone.<sup>16</sup> In contrast, the ester linkages do not contribute to the hydrogen-bonding. The urethane carbonyl stretching bands in BCMU with irregular hydrogen-bonding appear around 1720 cm<sup>−1</sup>, while hydrogen-bonded urethane carbonyl bands appear at a slightly lower wavenumber (about 1693 cm<sup>−1</sup>). The ester carbonyl stretching band remains around 1750 cm<sup>−1</sup>.

Parts A and B of Figure 6 give the transmission FT-IR spectra of the P-BPOD cast film and a 19-layer LB film at various polarization conditions. As shown in Figure 6A, the ester carbonyl stretching band in the cast film appears as a small peak at 1750 cm<sup>−1</sup>, while the C=O urethane stretching band is observed at 1720 cm<sup>−1</sup>. In the case of cast films, no change has been observed in these bands upon polarization, indicating no preferential orientation in the plane. However, the urethane C=O stretching bands in LB multilayers show two different bands (Figure 6B). One band sensitive to the polarization direction is due to the intramolecular hydrogen-bonding between neighboring urethane groups (1693 cm<sup>−1</sup>), indicating that C=O groups are oriented in the direction of the polymer chains aligned in the dipping direction. The other band (1720 cm<sup>−1</sup>) appears to be isotropic in the plane of the film and is attributed to irregular hydrogen bonds.

The carbonyl stretching band of the ordered region, which is due to the intramolecular hydrogen bonds, is very important in analyzing the orientation of the backbone because the vibrational direction of the carbonyl bonds occurs along the backbone. This carbonyl stretching band intensity varies with the degree of polarization. The intensity is observed to be much higher when the polarization is parallel rather than vertical to the dipping direction, while the intermediate intensity is observed without a polarizer. This further supports the preferential backbone orientation observed by UV/vis dichroism.

**Nonlinear Optical Properties.** As discussed previously, SH light is effectively generated when both the molecular hyperpolarizability is large and the molecules are noncentrosymmetrically packed.<sup>31</sup> Our LB system meets both of these requirements, where the pyrimidyl ring, as a weak electron-acceptor, induces the polarization into the asymmetric diacetylene core and the inherent Z-type deposition results in a noncentrosymmetric structure. Figure 7 gives SH intensities for both LB multilayers and cast films, which are measured at 60° incident angle by a Nd:YAG (1064 nm, pulse width 10 ns) fundamental laser beam. Both s- and p-polarized

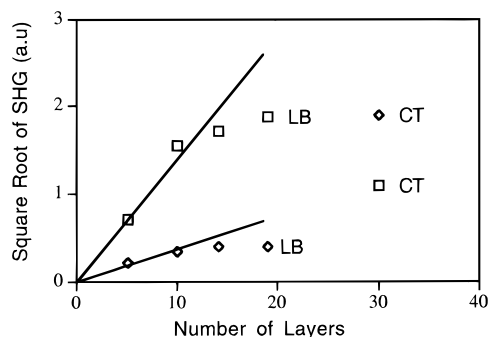


**Figure 7.** Second-harmonic generation for both s-p ( $\square$ ) and p-p ( $\diamond$ ) at  $60^\circ$  incident angle for LB 5, 10, 14, and 19 layers and cast film (CT).

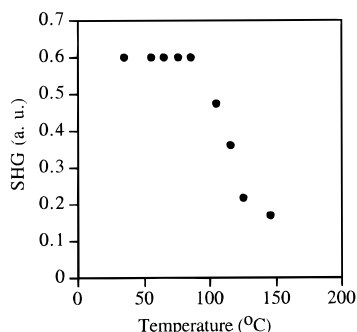


**Figure 8.** SHG intensity as a function of temperature.

beams (1064 nm) are incident on the samples, and only the p-polarized frequency-doubled beams (532 nm) are detected. We define  $I_{s-p}$  and  $I_{p-p}$  as p-polarized second harmonic intensity over incident s- and p-polarized fundamental beams, respectively.

As seen in Figure 7,  $I_{s-p}$  is found to be significantly larger than  $I_{p-p}$  in LB multilayers at  $60^\circ$  incident angle, whereas  $I_{p-p}$  is larger than  $I_{s-p}$  in cast films. It can be deduced that the origin of the SHG in LB films must be associated with the preferred backbone orientation and the net dipole moments for SHG are in the plane rather<sup>32,33</sup> than normal to the substrate. However, the dipole moments do not align in the same direction on the plane, because no SHG intensities were observed

at normal incidence. SHG measurements may be used to study the molecular ordering of the polar groups since any symmetric polar group structure gives no SHG signal. Typically, the asymmetric multilayers (Z-type) have been characterized by a linear increase of the square root of SHG with the number of layers.

We have observed that in Z-type P-BPOD LB films, the second harmonic intensity increases with the number of layers (Figure 7), indicating the highly ordered structure of P-BPOD LB films. In NLO systems where the absorption at the frequency-doubled region is not neglected,  $I_{2\omega}^{1/2}$  depends on  $Le^{-\alpha L}$  ( $\alpha L$ , absorbance times thickness  $L$ ). The effect of the exponential term is to decrease the SHG intensity and in thick films leads to saturation of SH intensity. The PDA LB films usually show strong absorption in the second harmonic region. However, for very thin films (up to a few layers) the exponential factor is sufficiently close to unity to give a linear dependence. As the film thickness increases, the exponential becomes significantly less than unity, leading to saturation behavior, as only the rear end of the film contributes to second harmonic generation. The optical density per layer measured in our films is 0.0105. This accounts for most of the decrease in the SHG signal. The small additional difference may be due to the incomplete alignment in thicker LB films. Since film thickness (below 400 Å) is much less than the coherence length (over 1  $\mu\text{m}$ ), the phase-matching conditions do not significantly affect the measurement. Absorption correction to the data was made for the p-polarized SH signal.

Improved second-order properties in ordered LB structures have been observed in 19-layer LB films. After absorption correction, a  $d$  coefficient obtained from the 19-multilayer film was 1.52 pm/V, which is significantly higher than that previously observed (0.3–0.5 pm/V in thickness of 0.2–0.3  $\mu\text{m}$ ) with the bulk self-assembled films.<sup>20</sup>  $I_{p-p}$  and  $I_{s-p}$  are in reverse order to what is seen for the bulk cast films. It was anticipated that the surprising asymmetry and order observed for the self-assembled bulk films will be further improved in Z-type LB films. What is observed is that while the asymmetry is maintained, the nature of molecular level order is entirely different. Figure 8 shows the thermal

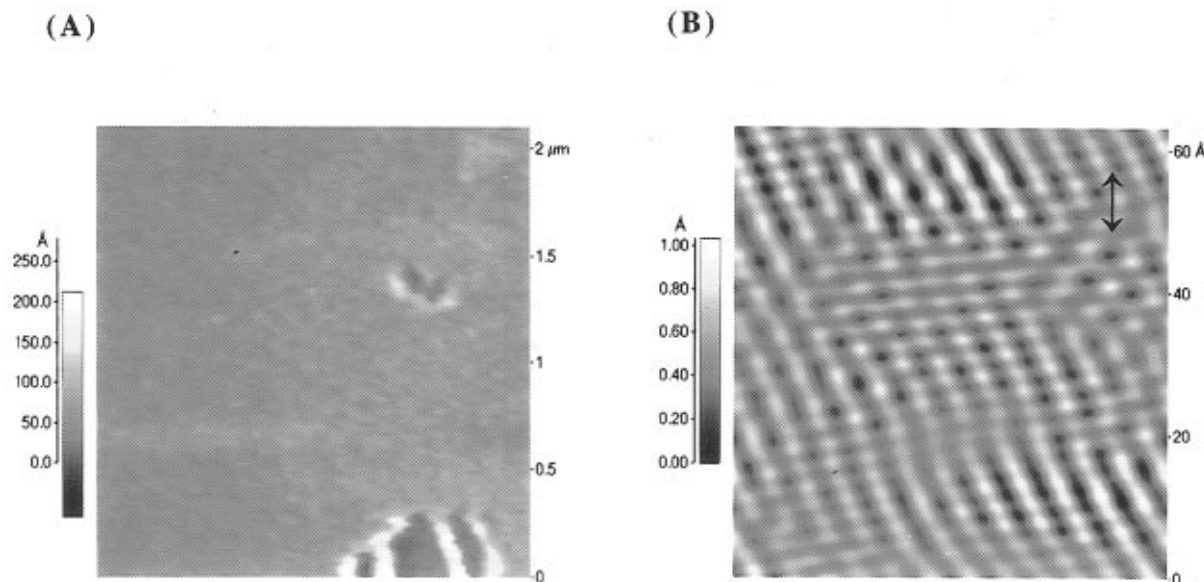


**Figure 9.** AFM images of LB 5 layers: left,  $2\ \mu\text{m} \times 2\ \mu\text{m}$  scale; right,  $600\ \text{nm} \times 600\ \text{nm}$  scale. Arrow indicates the dipping direction.

stability of SHG. SHG reduction occurred around 95 °C and implies disruption of the ordered structure due to the increased molecular mobility caused by the disruption of the H-bonding between the adjacent urethane moieties.<sup>20</sup> No SHG increase was found in the cooled sample after heating to 150 °C, indicating that the ordered structure of P-BPOD LB films may not be recovered.

We have carried out further studies toward polymer molecular orientation using the degenerate four-wave mixing (DFWM) technique<sup>21</sup> and AFM. The third-order nonlinear optical susceptibility (on-resonance) values measured for a 19-layer film at 532 nm were  $\chi^{(3)}_{||} \approx 4.0 \times 10^{-8}$  esu (polarization parallel to the dipping direction) and  $\chi^{(3)}_{\perp} \approx 5.9 \times 10^{-9}$  esu (polarization vertical to the dipping direction). This anisotropy of third-order nonlinearity appears to represent the preferable polymer chain orientation along the dipping direction. AFM was used to analyze the film morphology and molecular orientation of the surface. As can be seen in Figure 9, multilayer films in low magnification ( $2 \mu\text{m} \times 2 \mu\text{m}$ ) show irregular defects, such as pinholes and tearing, which may be formed during the vertical dipping process of rigid-rod molecules like the polydiacetylenes. The molecular resolution image ( $600 \text{ nm} \times 600 \text{ nm}$ ) from a selected area of the homogeneous surface (Figure 9B), which is filtered by using 2-D fast Fourier transform (FFT), shows the preferential backbone orientation (white region) along the dipping direction (in arrow) with the interchain spacing of around 5 Å.

## Conclusion

Preformed polydiacetylene has been deposited onto hydrophobic substrates to form NLO ultrathin films using the Langmuir–Blodgett (LB) film technique. Interestingly, the multilayer deposition by the dipping method resulted in asymmetric Z-type structures on hydrophobic substrates. Polarized UV/vis, FT-IR spectroscopy, and DFWM techniques indicated that the backbone is preferentially oriented along the dipping direction in the film plane with a mean fluctuation of  $\pm 30^\circ$ . SHG was found to increase with the number of layers and supports the presence of asymmetrically ordered Z-type films. Polarization-dependent SHG resulted in an  $I_{s-p}$  much larger than  $I_{p-p}$ , indicating that the dominant harmonic polarization is in the film plane rather than normal to it, in contrast to self-assembled bulk films. Both backbone orientation and Z-type film deposition provided the enhanced second- and third-order nonlinearities. The second-order nonlinear optical coefficient ( $d_{33}$ ) was determined to be 1.52 pm/V after absorption correction. AFM studies also supported backbone orientation along the dipping direction with an interchain spacing of about 5 Å.

**Acknowledgment.** We thank Mr. XinLi Jiang and Mr. F. J. Aranda for their help in SHG and DFWM measurements. We would like to thank Mr. S. Venkataramani for AFM images and Dr. K. S. Alva for academic discussions of relevant questions. Partial funding from ONR is gratefully acknowledged. The fourth sentence in the abstract is from the reviewer's comments.

## References and Notes

- (1) Zyss, J. *Molecular Nonlinear Optics, Materials, Physics, and Devices*; Academic Press, Inc.: New York, 1994.
- (2) Chemla, D. S.; Zyss, J. *Nonlinear Optical Properties of Organic Molecules and Crystals*; Academic Press, Inc.: New York, 1987; Vols 1 and 2.
- (3) Prasad, P. N.; Williams, D. J. *Introduction to Nonlinear Optical Effects in Molecules and Polymers*; John Wiley & Sons, Inc.: New York, 1991.
- (4) Ulman, A. *An Introduction to Ultrathin Organic Films—from Langmuir–Blodgett to Self-Assembly*; Academic Press, Inc.: New York, 1991.
- (5) Popovitz-Bird, R.; Hung, D. J.; Shavit, E.; Lahav, M.; Leiserowitz, L. *Thin Solid Films* **1989**, *178*, 203.
- (6) Ashwell, G. J.; Jackson, P. D.; Crossland, W. A. *Nature* **1994**, *368*, 438.
- (7) Watakabe, A.; Okada, H.; Kunitake, T. *Langmuir* **1994**, *10*, 2722.
- (8) Anderson, B. L.; Hoover, J. M.; Lindsay, G. A.; Higgins, B. G.; Stroeve, P.; Kowel, S. T. *Thin Solid Films* **1989**, *179*, 413.
- (9) Young, M. C. J.; Lu, W. X.; Tredgold, R. H.; Hodge, P.; Abbasi, F. *Electron. Lett.* **1990**, *26* (14), 993.
- (10) Carr, N.; Goodwin, M. J.; McRoberts, A. M.; Gray, G. W.; Marsden, R.; Scowston, M. *Makromol. Chem., Rapid Commun.* **1987**, *8*, 487.
- (11) Tieke, B.; Wegner, G.; Naegele, D.; Ringsdorf, H. *Angew. Chem., Int. Ed. Engl.* **1976**, *15*, 764.
- (12) Tieke, B.; Graf, H. J.; Wegner, G.; Naegele, B.; Ringsdorf, H.; Banerjee, S.; Day, D.; Lando, J. B. *Colloid. Polym. Sci.* **1977**, *225*, 521.
- (13) Tieke, B.; Weiss, K. *J. Colloid Interface Sci.* **1984**, *101* (1), 129.
- (14) Carter, G. M.; Chen, Y. J.; Georger, J., Jr.; Hryniewicz, J.; Rooney, M.; Rubner, M. F.; Samuelson, L. A.; Sandman, D. J.; Thakur, M.; Tripathy, S. K. *Mol. Cryst. Liq. Cryst.* **1984**, *106*, 259.
- (15) Wegner, G. *Z. Naturforsch.* **1969**, *24B*, 824.
- (16) Bloor, D.; Chance, R. R. *Polydiacetylenes*; Martinus Nijhoff: Boston, 1985; pp 239–256.
- (17) Garito, A. F.; Teng, C. C.; Wong, K. Y.; Zammani-Khamiri, O. *Mol. Cryst. Liq. Cryst.* **1984**, *106*, 219.
- (18) Berkovic, G.; Superfine, R.; Guyot-Sionnest, P.; Shen, Y. R.; Prasad, P. N. *J. Opt. Soc. Am. B* **1988**, *5* (3), 668.
- (19) Kim, W. H.; Kodali, N. B.; Kumar, J.; Tripathy, S. K. *Macromolecules* **1994**, *27*, 1819.
- (20) Kim, W. H.; Bihari, B.; Moody, R.; Kodali, N. B.; Kumar, J.; Tripathy, S. K. *Macromolecules* **1995**, *28*, 642.
- (21) Rao, D. V. G. N.; Aranda, Francisco J.; Roach, J. F.; Remy, D. *Appl. Phys. Lett.* **1991**, *58* (12), 1241.
- (22) Biegajski, J. E.; Burzynski, R.; Cadenhead, D. A.; Prasad, P. N. *Macromolecules* **1986**, *19*, 2457.
- (23) Byrd, H.; Pike, J. K.; Talham, D. R. *Chem. Mater.* **1993**, *5*, 709.
- (24) Schwiegk, S.; Vahlenkamp, T.; Xu, Y.; Wegner, G. *Macromolecules* **1992**, *25*, 2513.
- (25) Ren, Y.; Liu, W.; Han, M.; Gao, M.; Zhao, Y.; Li, T.; Yang, J. *Thin Solid Films* **1993**, *229*, 249.
- (26) Seki, T.; Sakuragi, M.; Kawanishi, Y.; Suzuki, Y.; Tamaki, T.; Fukuda, R. I.; Ichimura, K. *Langmuir* **1993**, *9*, 211.
- (27) Sauer, T.; Arndt, T.; Batchelder, D. N.; Kalachev, A. A.; Wegner, G. *Thin Solid Films* **1990**, *187*, 357.
- (28) Barnik, M. I.; Palto, S. P.; Khavrichiev, V. A.; Shtykov, N. M.; Yudin, S. G. *Thin Solid Films* **1989**, *179*, 493.
- (29) Cammarata, V.; Atanasoska, L.; Miller, L. L.; Kolaskie, C. J.; Stallman, B. J. *Langmuir* **1992**, *8*, 876.
- (30) Vandevyver, M.; Barraud, A.; Teixier, R. *J. Colloid Interface Sci.* **1982**, *85* (2), 571.
- (31) (a) Schoondorp, M. A.; Schouten, A. J.; Hulshof, J. B. E.; Feringa, B. L. *Langmuir* **1993**, *9*, 1323. (b) Decher, G.; Tieke, B.; Bosshard, C.; Gunter, P. *J. Chem. Soc., Chem. Commun.* **1988**, 933.
- (32) Wijekoon, W. M. K. P.; Karna, S. P.; Talapatra, G. B.; Prasad, P. N. *J. Opt. Soc. Am. B* **1993**, *10* (2), 213.
- (33) Su, W.-F. A.; Kurata, T.; Nobutoki, H.; Koezuka, H. *Langmuir* **1992**, *8*, 915.

MA951214H